Proper development of relay somatic sensory neurons and D2/D4 interneurons requires homeobox genes *Rnx*/*Tlx-3* and *Tlx-1*

Ying Qian,[1,2] Senji Shirasawa,[3] Chih-Li Chen,[1,2] Leping Cheng,[1,2] and Qiufu Ma[1,2,4]

[1]The Dana-Farber Cancer Institute and [2]Department of Neurobiology, Harvard Medical School, Boston, Massachusetts 02115, USA; [3]Department of Pathology, International Medical Center of Japan, Tokyo 162-8655, Japan

Trigeminal nuclei and the dorsal spinal cord are first-order relay stations for processing somatic sensory information such as touch, pain, and temperature. The origins and development of these neurons are poorly understood. Here we show that relay somatic sensory neurons and D2/D4 dorsal interneurons likely derive from *Mash1*-positive neural precursors, and depend on two related homeobox genes, *Rnx* and *Tlx-1*, for proper formation. Rnx and Tlx-1 maintain expression of *Drg11*, a homeobox gene critical for the development of pain circuitry, and are essential for the ingrowth of trkA+ nociceptive/thermoceptive sensory afferents to their central targets. We showed previously that *Rnx* is necessary for proper formation of the nucleus of solitary tract, the target for visceral sensory afferents. Together, our studies demonstrate a central role for *Rnx* and *Tlx-1* in the development of two major classes of relay sensory neurons, somatic and visceral.

[*Key Words*: Rnx; Tlx-1; MASH1; DRG11; trkA; somatic sensory; D2; D4 interneurons]

Received February 6, 2002; revised version accepted April 1, 2002.

Processing of most sensory information is conveyed through relay sensory stations in the hindbrain and spinal cord. In the cranial region, somatic sensory functions, such as the senses of touch, pain, and temperature, are relayed through the trigeminal nuclei (nTG), whereas sensory information from internal organs is conveyed through the nucleus of solitary tract (nTS) (Saper 2000; Fig. 1A). At the trunk level, mechanoceptive and nociceptive/thermoceptive sensory afferents project to the deep and superficial laminae of the dorsal spinal cord, respectively (Snider 1994).

The development of various relay sensory neurons is only beginning to be understood. We recently demonstrated that the nTS derives from a dorsal column of precursors that express the proneural gene *Mash1* (Qian et al. 2001). All newly formed nTS neurons coexpress two homeobox genes, *Rnx* and *Phox2b*, with *Rnx* being necessary for proper development of these neurons (Qian et al. 2001). However, the origin and identity of the cells fated to form the nTG are still unclear, despite the fact that for many years the trigeminal system has been used as a model for studying neural development and neurophysiology (Davies 1988).

In the spinal cord, *Drg11*, a paired class of homeobox gene (Saito et al. 1995), was recently shown to be required for proper development of the superficial laminae of the dorsal horn (Chen et al. 2001). Also, several classes of "dorsal interneurons" have been characterized, including D0, D1, D2, D3, and D4, which are defined by expression of *Lbx1*, *Lh2*, *Isl1*, *Lim1/2*, and *Lmx1b*, respectively (Tsuchida et al. 1994; Liem et al. 1997; Helms and Johnson 1998; Lee et al. 1998; Bermingham et al. 2001; Gowan et al. 2001; Moran-Rivard et al. 2001; Pierani et al. 2001). Along the dorsoventral axis, neural precursors in the dorsal neural tube are subdivided into three compartments that are based on complementary expression of the proneural genes *Math1*, *ngn1/2*, and *Mash1* (Ma et al. 1997; Helms and Johnson 1998; Gowan et al. 2001). D1 interneurons and a portion of D3 interneurons develop from the dorsal regions of the ventricular zone that express *Math1* and *ngn1*, respectively (Helms and Johnson 1998; Bermingham et al. 2001; Gowan et al. 2001). However, little is known about the origins and molecular control of the formation of D2 and D4 interneurons. The origin of *Drg11*-positive neurons and the fates of *Mash1*-positive precursors are also poorly understood.

The *Tlx* family of homeobox genes contains three members, *Tlx-1/Hox11*, *Enx/Hox11-L1/Tlx-2*, and *Rnx/Hox11L2/Tlx-3* (Dube et al. 1991; Hatano et al. 1991; Kennedy et al. 1991; Dear et al. 1993, 1995; Raju et al. 1993; Roberts et al. 1994; Hatano et al. 1997; Shirasawa et al. 1997, 2000; Logan et al. 1998; Tang et al. 1998). In

[4]Corresponding author.
E-MAIL Qiufu_Ma@dfci.harvard.edu; FAX (617) 632-4595.
Article and publication are at http://www.genesdev.org/cgi/doi/10.1101/gad.982802.

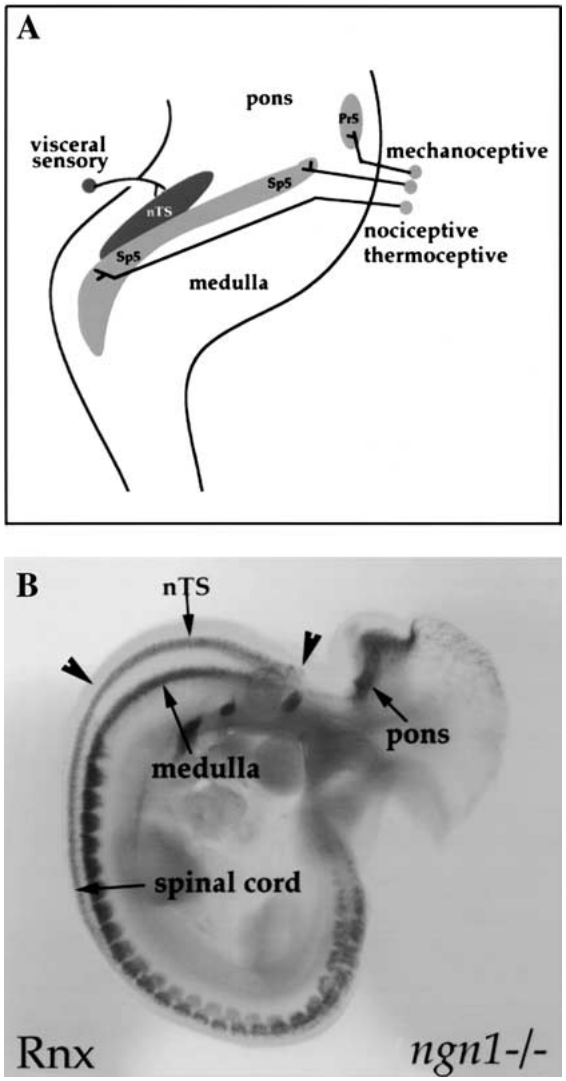

Figure 1. (*A*) A schematic of the cranial somatic and visceral sensory nervous system. The visceral sensory afferents, corresponding to the distal components of the VIIth, IXth, and Xth nerves, project to the nucleus of solitary tract (nTS) in the hindbrain. Mechanosensory neurons in the trigeminal ganglia innervate the principle trigeminal nucleus (Pr5) and the spinal trigeminal nuclei (Sp5). The thermoceptive and nociceptive sensory afferents from the trigeminal ganglia and the proximal components of the VIIth, IXth, and Xth nerves project to the superficial laminae of the caudal Sp5. (*B*) *Rnx* expression in E11.5 mouse embryos. An *ngn1* mutant embryo was chosen for a better view of *Rnx* expression in the developing central nervous system, due to absence of all somatic sensory ganglia and vestibular ganglia in *ngn1* mutants (Ma et al. 1998). Part of this picture was published previously (Qian et al. 2001). The medullary portion of the dorsal stripe (flanked by arrowheads) is fated to form the nTS (Qian et al. 2001). Fates of other *Rnx*-expressing cells in the developing pons, medulla and spinal cord are investigated in the present study.

the developing hindbrain and spinal cord, *Rnx* and *Tlx-1* are initially expressed in longitudinal columns of cells, extending through the hindbrain and spinal cord (Fig. 1B; Logan et al. 1998), but the expression pattern becomes quite complex at later developmental stages (Logan et al. 1998; Qian et al. 2001; see below).

Here we show that *Rnx* and *Tlx-1* are associated with sequential development of multiple classes of neurons throughout the developing hindbrain and spinal cord. In addition to giving rise to the nTS and (nor)adrenergic centers (Qian et al. 2001), we show that early born *Rnx*-expressing cells, derived from a subset of *Mash1*-positive precursor cells, are fated to form D2 and D4 interneurons. We then show that late born *Rnx*-expressing cells, derived from the entire dorsoventral extent of *Mash1*-positive domain, form first-order relay somatic sensory neurons, including the trigeminal nuclei and the superficial laminae of the dorsal spinal cord. Analyses of *Rnx* and *Tlx-1* single and double mutants show that the proper development of D2/D4 interneurons and relay somatic sensory neurons is dependent on *Rnx* or *Tlx-1*. Our studies provide a molecular model for the sequential formation of distinct classes of relay sensory neurons in the developing hindbrain and spinal cord.

Results

Rnx-*expressing cells likely develop from MASH1-positive neural precursors*

In the developing hindbrain and spinal cord, *Rnx* is initially expressed in two longitudinal columns of cells in E10.5–E11.5 mouse embryos (Figs. 1B, 2B; Qian et al. 2001), and the expression then becomes continuous in E12.5 embryos (Fig. 2E). We showed previously that dorsally derived *Rnx*-expressing cells in E10.5–E11.5 medulla likely develop from MASH1-positive precursors (Qian et al. 2001). To determine the origins of the remaining *Rnx*-expressing cells, we again compared *Rnx* expression with that of two neural precursor markers, NGN1 and MASH1. Double staining of *Rnx* mRNA and MASH1 protein shows that in the spinal cord (Fig. 2B–D) of E11.5 wild-type embryos, the dorsal and ventral stripes of *Rnx*-expressing cells are located precisely at the lateral edges of the most dorsal and most ventral portions of the MASH1-positive domain, respectively (Fig. 2B, arrowheads). A few cells show codetection of *Rnx* mRNA and MASH1 protein (Fig. 2C,D, arrows), whereas no NGN1-positive cells, which are located dorsal to MASH1-positive territory, coexpress *Rnx* (data not shown).

In E12.5 spinal cord, the dorsoventral limits of *Rnx*-expressing cells again coincide perfectly with that of MASH1-positive territory (Fig. 2F, arrowheads). At this stage, multiple layers of cells at the lateral edge of MASH1-positive territory show double staining of MASH1 protein and *Rnx* mRNA (Fig. 2F,G, arrows). Note that instead of the columnar organization seen in E10.5–E11.5 embryos (Fig. 2A,B), the entire dorsoventral extent of MASH1-positive territory forms *Rnx*-expressing cells in E12.5 embryos (Fig. 2F). Again, no adjacent NGN1-positive cells coexpress *Rnx* in E12.5 embryos (Fig. 2H, arrows). Since Math1-positive precursors are located further dorsal to NGN1-positive cells (Helms and Johnson 1998; Gowan et al. 2001), we reasoned that they

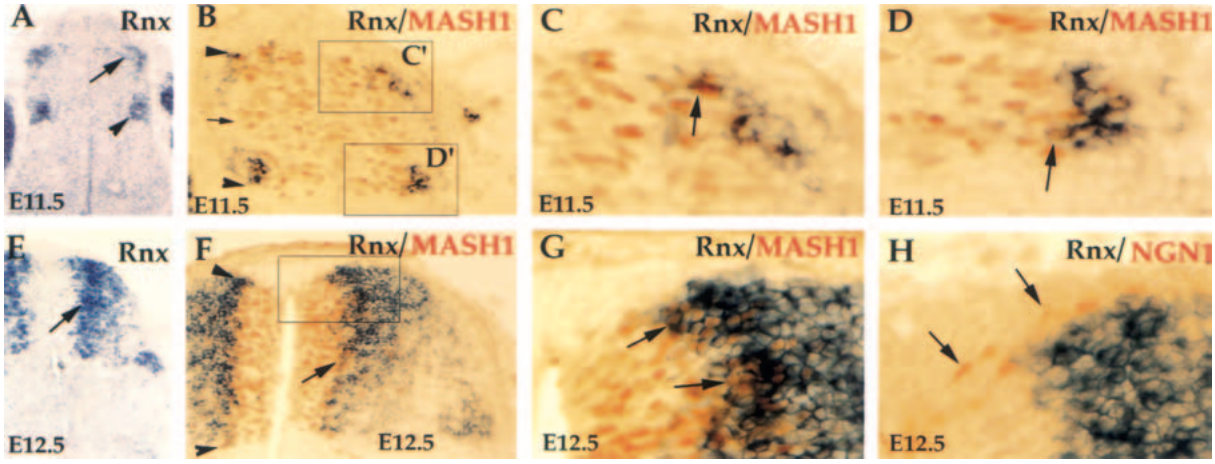

Figure 2. *Rnx*-positive neurons likely develop from *Mash1*-positive precursors. Transverse sections through spinal cord at the lumbar level of E11.5 (*A–D*) and E12.5 (*E–G*) wild-type embryos. Panels *A* and *E* show in situ hybridization with *Rnx* as the probe. Panels *B–D* and *F–H* show double staining, with *Rnx* mRNA (purple) detected by in situ hybridization, and MASH1 (*B–D*,*F*,*G*, brown) or NGN1 (*F*, brown) proteins detected by immunostaining with anti-MASH1 or NGN1 antibodies. *B* and *F* show the dorsal neural tube, and *C*, *D*, and *G* are higher magnification of the boxed regions shown in *B* and *F*, respectively. *H* is from an adjacent section of *F* and roughly corresponds to the boxed region shown in *F*.

should also not coexpress *Rnx*. Identical results are seen in the caudal developing medulla (data not shown). These studies suggest that both early and late born *Rnx*-positive cells may develop exclusively from *Mash1*-positive precursors.

Development of D2 interneurons in the spinal cord is dependent on Rnx

In E10.5–E11.5 mouse embryos, the dorsal column of *Rnx*-expressing cells spans from the medulla to the caudal spinal cord in E10.5–E11.5 mouse embryos (Fig. 1B). In chick spinal cord, dorsal *Rnx*-expressing cells correspond to D2 interneurons, as indicated by coexpression of *Rnx/Tlx-3* and *Isl1* (Logan et al. 1998). *Isl1* is a marker for D2 interneurons (Tsuchida et al. 1994). Consistently, we found that *Isl1* expression is lost in the dorsal spinal cord of E11.5 *Rnx* mutant mouse embryos (Fig. 3, cf. B and C, arrows), suggesting that *Rnx* function is necessary for D2 interneuron development. In contrast, *Isl1* expression in the dorsal root ganglia (Fig. 3, cf. B and C, "DRG") and ventral motor neurons (Fig. 3, cf. B and C, "mn") is not affected in *Rnx* deficient mice.

The ventral column of Rnx*-expressing cells corresponds to D4 interneurons*

The ventral column of *Rnx*-expressing cells extends from the pons to the caudal spinal cord in E10.5–E11.5 embryos (Fig. 1B). The following data indicate that ventrally derived *Rnx*-expressing cells in the medulla and spinal cord correspond to D4 interneurons, which are previously defined by expression of the lim-homeobox gene, *Lmx1b* (Tsuchida et al. 1994).

In the medulla of E11.5 wild-type embryos, both *Lmx1b* and *Rnx* are expressed in two stripes of cells along the dorsoventral axis (Fig. 4A,B, red and black arrows). Within the ventral column, expression of *Rnx* and *Lmx1b* is detected in a cluster of cells adjacent to the ventricular zone (Fig. 4A,B, black arrowheads), and in a string of cells that appear to be migrating laterally and ventrally (Fig. 4A,B, black arrows). Two-color in situ hybridization shows that *Rnx* and *Lmx1b* are coexpressed

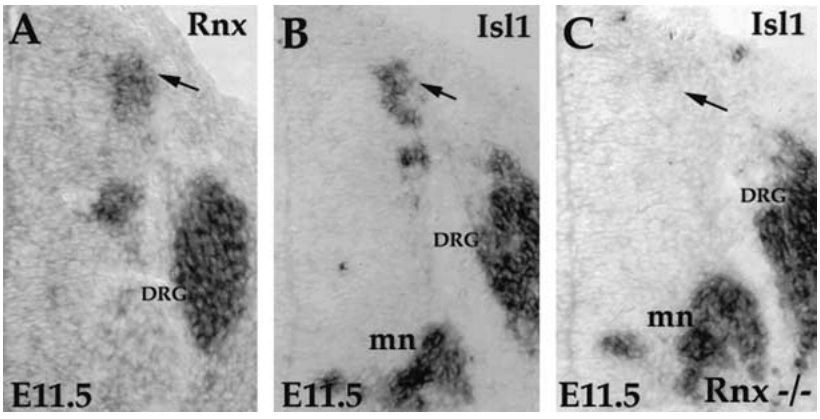

Figure 3. A requirement of *Rnx* for formation of D2 interneurons. Sections through the spinal cord of E11.5 wild-type (*A*,*B*) and *Rnx*-deficient (*C*) embryos. In situ hybridization was performed with indicated probes. Note that in *Rnx* mutant embryos, *Isl1* expression is absent in dorsally derived cells (cf. *B* and *C*, arrows), but normal in the ventral motor neurons (cf. *B* and *C*, "mn") and in the dorsal root ganglia (cf. *B* and *C*, "DRG").

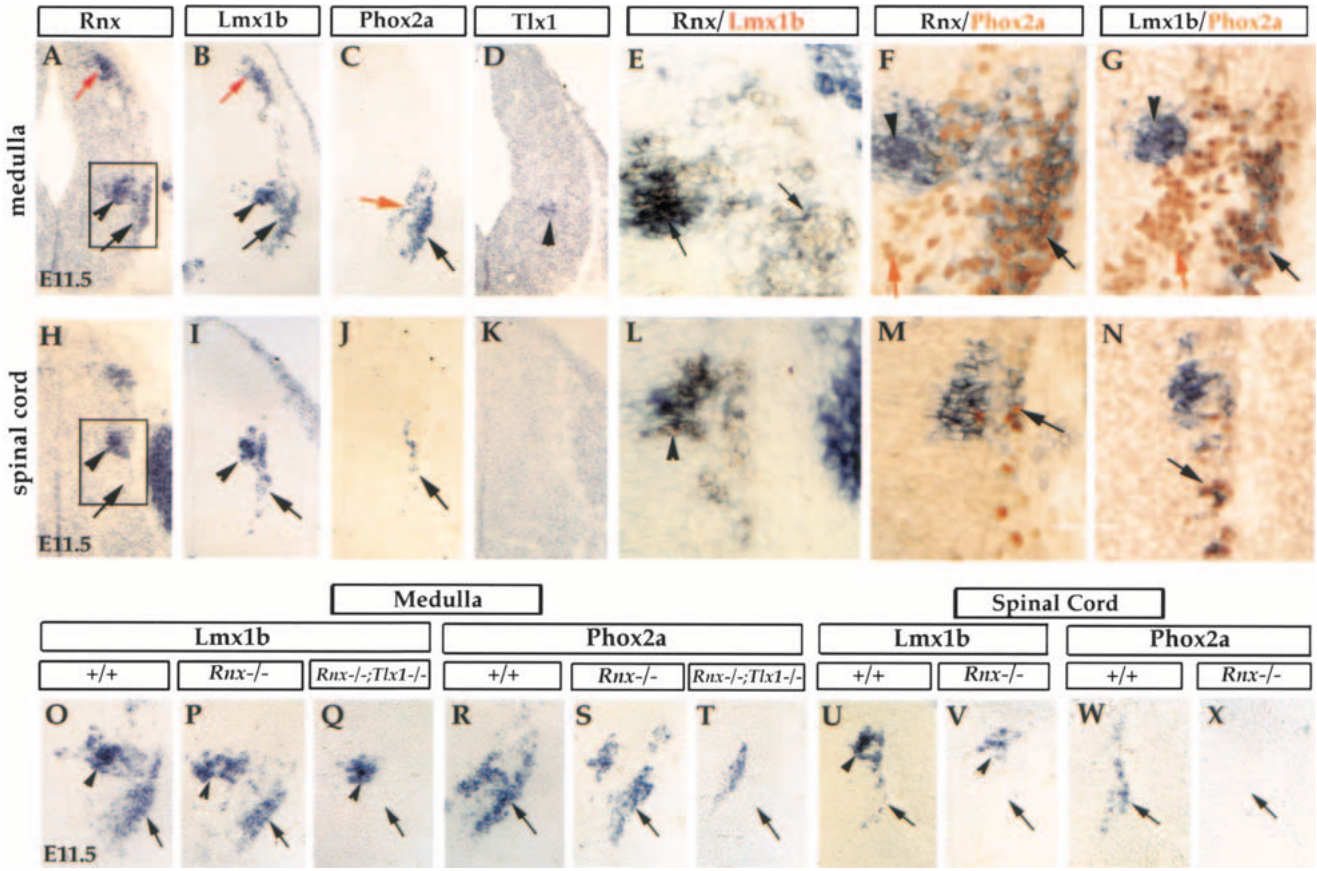

Figure 4. Expression in and function of *Rnx* and *Tlx-1* in formation of D4 interneurons. (*A–N*) Expression of *Rnx*, *Tlx-1*, *Lmx1b*, and *Phox2a* in D4 interneurons. Sections through the medulla (*A–G*) and the hindlimb bud level spinal cord (*H–N*) of E11.5 wild-type embryos. Panels *E*–G and panels *L–N* are equivalent to the boxed regions shown in panel *A* and *H*, respectively. *A–D* and *H–K* are in situ hybridization with indicated probes. Panels *E* and *L* show double color in situ hybridization of *Rnx* (purple) and *Lmx1b* (brown). Panels *F–G* and *M–N* show double staining of *Rnx* or *Lmx1b* mRNA in the cytoplasm (purple) and Phox2a protein in the nucleus (brown). (*O–X*) Loss of *Lmx1b* and *Phox2a* expression in prospective D4 interneurons in *Rnx* and *Tlx-1* single or double mutants. Transverse sections through medulla (*O–T*) and spinal cord (*U–X*) of E11.5 wild-type (*O,R,U,W*), *Rnx* single mutant (*P,S,V,X*), and *Rnx/Tlx-1* double mutant (*Q,T*) embryos. Panels *O–T* and panels *U–X* are equivalent to the boxed regions shown in *A* and *H*, respectively. In situ hybridization was performed with indicated probes.

in these cells (Fig. 4E, arrows), indicating that these cells correspond to the previously described D4 interneurons. Expression of another *Tlx* family member, *Tlx-1*, is restricted exclusively to the medial area where *Rnx* appears to be expressed (Fig. 4, cf. A and D, arrowheads). Coexpression of *Rnx* and *Tlx-1* is further inferred from the requirement of both genes for development of D4 interneurons (see below). *Phox2a*, a *Phox2b*-related gene (Valarché et al. 1993; Yokoyama et al. 1996; Pattyn et al. 1997), is expressed in two groups of cells, a medial string of unknown cells (Fig. 4C, red arrow) and the laterally localized cells (Fig. 4C, black arrow). The latter group corresponds to D4 interneurons, as demonstrated by co-detection of Phox2a protein and *Lmx1b* or *Rnx* mRNA in these cells (Fig. 4F,G, arrows). Note that Phox2a is not coexpressed with *Rnx* or *Lmx1b* in the medial cluster of cells (Fig. 4F,G, arrowheads).

An analogous expression pattern is observed in the developing spinal cord. At the hindlimb bud level, the ventral column of *Rnx*-expressing cells (Fig. 4H, arrowhead) again corresponds to prospective D4 interneurons, as indicated by coexpression of *Rnx* and *Lmx1b* in a cluster of cells within the mantle zone in E11.5 embryos (Fig. 4H,I,L, arrowheads). These cells apparently migrate ventrally, and later start to express *Phox2a* (Fig. 4J, arrow) plus *Lmx1b* (Fig. 4I, arrow), whereas *Rnx* expression has probably been down-regulated (Fig. 4H, arrow). Double labeling shows that a few cells still coexpress *Rnx* and *Phox2a* (Fig. 4M, arrow), while most *Phox2a*-positive cells coexpress *Lmx1b* (Fig. 4N, arrow). We conclude that spinal D4 interneurons first express *Rnx* and *Lmx1b*, and then *Lmx1b* and *Phox2a*.

Rnx *and* Tlx-1 *are required for proper formation of D4 interneurons*

To determine the roles of *Rnx* and *Tlx-1* during development of D4 interneurons, we analyzed *Rnx* and *Tlx-1* single or double mutants (Roberts et al. 1994; Shirasawa et al. 2000). In the medulla of E11.5 *Rnx/Tlx-1* double

mutants, expression of both *Lmx1b* and *Phox2a* is eliminated in the lateral area (Fig. 4, cf. O and Q; R and T, arrows). In contrast, *Lmx1b* expression in the dorsal medial area is normal in double mutants (Fig. 4, O and Q, arrowheads), and no defect is detected in *Rnx* or *Tlx-1* single mutants (Fig. 4, cf. O and P; R and S; data not shown). In the caudal spinal cord, expression of *Lmx1b* and *Phox2a* in ventrally migrating D4 interneurons is already eliminated in *Rnx* single mutants (Fig. 4, cf. U and V; W and X, arrows), consistent with a lack of strong *Tlx-1* expression at this axial level (data not shown). Again, the most dorsal *Lmx1b* expression is unperturbed in *Rnx* single (Fig. 4V, arrowhead) or *Rnx*/*Tlx-1* double mutants (data not shown). As no cell death was detected by TUNEL assay (see below, Fig. 7), we conclude that initiation of *Lmx1b* expression in prospective D4 interneurons is independent of *Rnx* or *Tlx-1*, but late expression of both *Lmx1b* and *Phox2a* requires either *Rnx* or *Tlx-1*.

Late born Rnx*-expressing cells are fated to form the trigeminal nuclei and the dorsal horn of the spinal cord*

As described in Figure 2E, *Rnx*-expressing cells in E12.5 embryos no longer show a columnar pattern. Our data, detailed in the following section, show that the late born cells are fated to form first-order relay somatic sensory stations, including the trigeminal nuclei and the superficial laminae of the dorsal spinal cord.

In the developing pons, the earliest born *Rnx*-expressing cells seen in E10.5 mouse embryos coexpress *Phox2a* and/or *Phox2b* and develop into (nor)adrenergic neurons (Qian et al. 2001). By E11.5, while *Rnx* expression has been down-regulated in prospective (nor)adrenergic neurons (Qian et al. 2001), a large number of new *Rnx*-expressing cells emerge, most of which do not express either *Phox2b* or *Phox2a* (Fig. 5A, arrow; data not shown). At E14.5 and E16.5, the *Rnx*-positive, *Phox2*-negative cells are located in a ventral lateral area of the developing pons corresponding to the principle trigeminal nucleus (Pr5) (Fig. 5B,C, arrows). Interestingly, most neurons in the Pr5 express *Drg11* (Fig. 5D, arrow). Note that *Drg11* is also expressed in regions surrounding the Pr5, where *Rnx* is not expressed (Fig. 5, cf. C and D, arrowheads).

Similarly, in the caudal medulla at E12.5, a new group of *Rnx*-positive, *Phox2*-negative cells is observed that spans most of the dorsal medulla (Fig. 5E). By E14.5, these neurons are restricted to the dorsal lateral region corresponding to the spinal trigeminal nucleus (Sp5) (Fig.

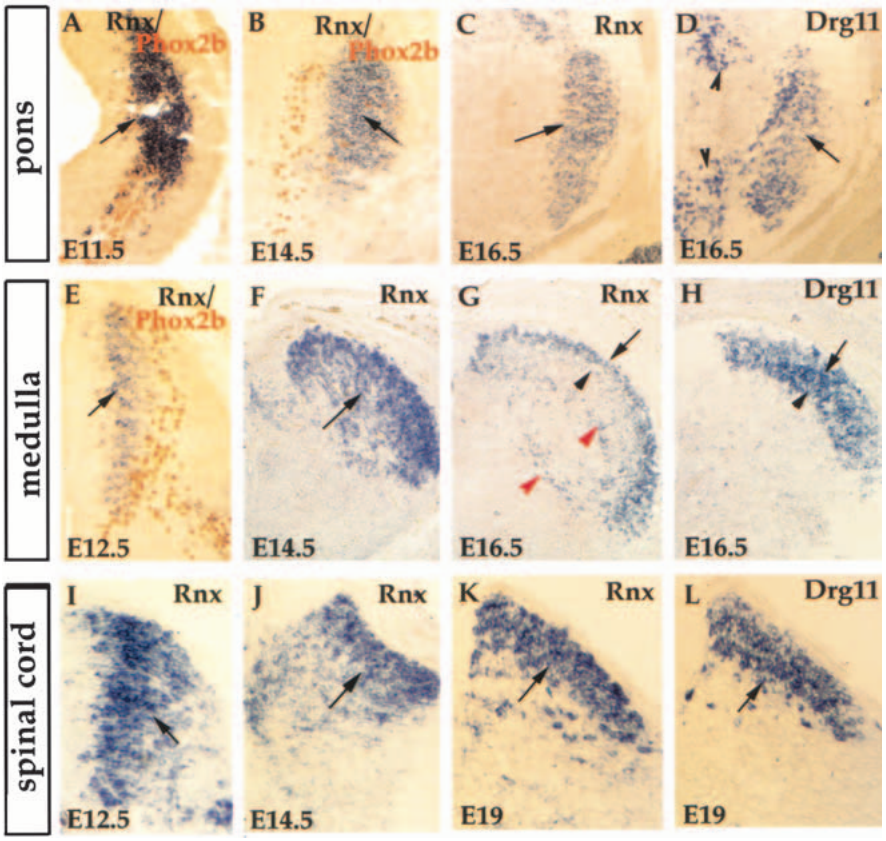

Figure 5. *Rnx* expression in the developing relay somatic sensory neurons. Transverse sections through pons (*A–D*), medulla (*E–H*), and spinal cord (*I–L*) of embryos at indicated stages. In situ hybridization was performed with indicated probes (*C*,*D*,*F–L*). Panels *A*, *B*, and *E* are double staining of *Rnx* mRNA (purple) and *Phox2b* protein (brown). Note that in E11.5 pons and E12.5 medulla, most newly formed *Rnx*-expressing cells no longer coexpress *Phox2b* or *Phox2a* (*A* and *E*, arrows), which are seen more clearly at high magnification (data not shown).

5F, arrow). At E16.5, *Rnx* expression in the caudal Sp5 shows a lamina-specific pattern, with predominant expression detected in the superficial laminae (Fig. 5G, arrow) and two deep laminae (Fig. 5G, red arrowheads). In contrast, *Drg11* expression is restricted to the superficial portion of the Sp5 (Fig. 5H, arrow), and extends to a deeper zone in comparison with the superficial *Rnx* expression (Fig. 5, cf. G and H, black arrowheads). Because *Drg11* expression in the Sp5 is dependent on *Rnx* (see below), *Rnx* expression is likely to have been down-regulated in *Drg11*-positive, *Rnx*-negative zone. No *Phox2b* expression is detected in the Sp5 (data not shown). *Drg11* is expressed weakly and transiently in the developing nTS, where *Phox2b* is strongly and persistently expressed (Qian et al. 2001; data not shown).

In E14.5 developing spinal cord, late born *Rnx*-expressing cells are restricted to the dorsal horn of the spinal cord (Fig. 5J, arrow). By E19, *Rnx* expression is primarily observed in the superficial laminae (Fig. 4K, arrow). Again, *Drg11* (Fig. 4L, arrows), but not *Phox2b* (Pattyn et al. 1997; data not shown), is expressed in the dorsal spinal cord.

Rnx *and* Tlx-1 *are required for proper differentiation of relay somatic sensory neurons*

To determine the role of *Rnx* and *Tlx-1* in the development of relay somatic sensory neurons, we further analyzed single and double mutant embryos. We found that *Drg11* expression is eliminated in E14.5 Sp5 and E16.5 dorsal horn of the spinal cord in *Rnx*/*Tlx-1* double mutants (Fig. 6, cf. A and C; D and F, arrows). Partial loss of *Drg11* expression is observed in *Rnx* single mutants (Fig. 6, cf. A and B; D and E, arrows), whereas no defect is detected in *Tlx-1* single mutants (data not shown). The situation in the developing Pr5 is a bit different. *Drg11* expression in this nucleus is not affected in *Rnx* or *Tlx-1* single mutants (Fig. 6, cf. G and H, arrows; data not shown), and is only partially reduced in *Rnx*/*Tlx-1* double mutants (Fig. 6, cf. G and I, arrows). The partial dependence of Pr5 development on *Rnx*/*Tlx-1* is reminiscent of the partial requirement of *Rnx* for formation of another pons structure, the locus ceruleus (Qian et al. 2001).

Expression of two additional markers, *Ebf3* and *Lmx1b*, was also affected in *Rnx*/*Tlx-1*-deficient mice. *Ebf3* is a basic helix-loop-helix gene expressed in the superficial laminae of the spinal cord (Fig. 6J, arrow) and the Sp5 (data not shown; Garel et al. 1997; Wang et al. 1997). *Ebf3* expression in these two structures is absent in *Rnx*/*Tlx-1* double mutants (Fig. 6, cf. J and K, arrows; data not shown), and it is greatly reduced in *Rnx* single mutants (data not shown) at E14.5 or later stages. *Lmx1b* is initially expressed in D4 interneurons (Fig. 4), but the expression is expanded to the dorsal horn of the spinal cord at later stages (Fig. 6L, arrow). In E14.5 *Rnx*/*Tlx-1* double mutants, *lmx1b* expression is still restricted to the dorsal spinal cord (Fig. 6M, arrow). However, instead of the nearly uniform expression seen in wild-type embryos, many cells within the superficial laminae show a

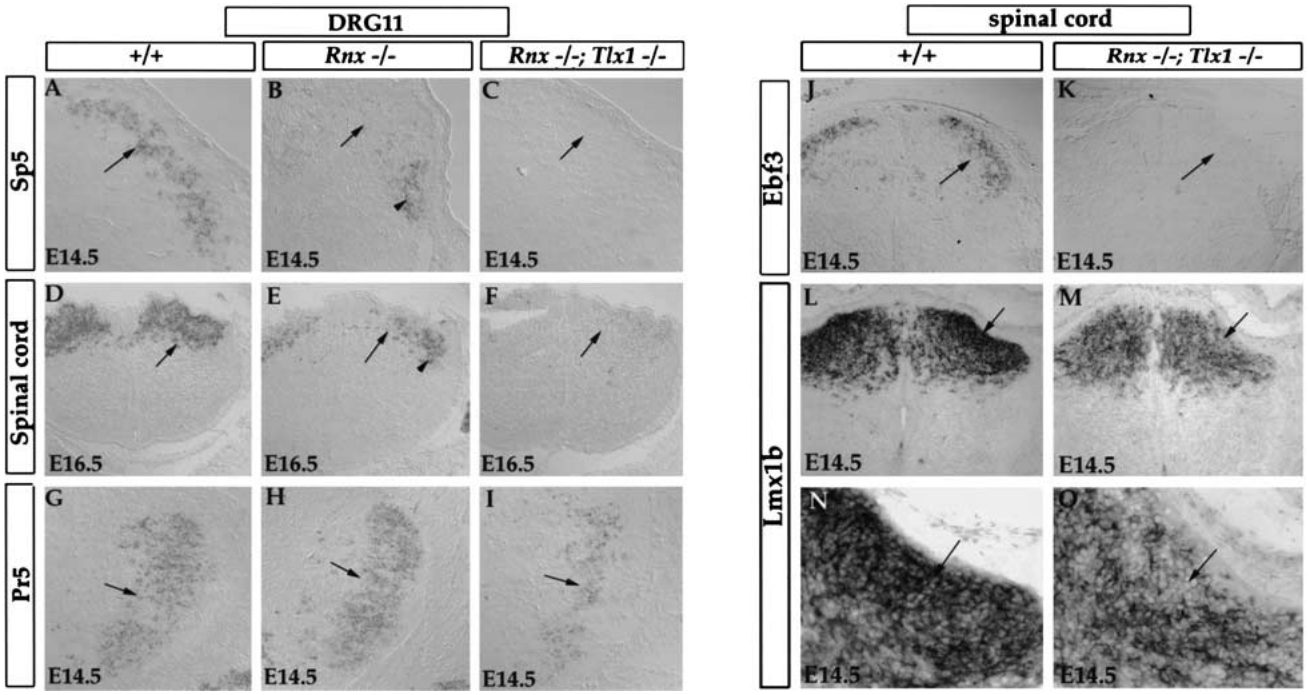

Figure 6. Loss or reduction of *Drg11*, *Ebf3*, and *Lmx1b* expression in relay somatic sensory neurons in *Rnx* and *Tlx-1* single or double mutants. Transverse sections through the spinal trigeminal nucleus (Sp5) (*A–C*, arrows), the spinal cord (*D–F*, and *J–O*), and the principle trigeminal nucleus (Pr5) (*G–I*, arrows) of embryos with indicated genotypes and developmental stages. In situ hybridization was performed with indicated probes. *N* and *O* are higher magnification of the dorsal horn shown in panels *L* and *M*, respectively.

reduction of *Lmx1b* expression in *Rnx*/*Tlx-1* double mutants (Fig. 6, cf. N and O, arrows).

Examination of embryos at earlier stages shows that initiation of *Drg11* and *Ebf3* expression is independent of *Rnx* or *Tlx-1*, as indicated by their normal expression in E12.5 *Rnx*/*Tlx-1* double mutants (Fig. 7, cf. A and B, arrows; data not shown). Significant loss of *Drg11* and *Ebf3* expression is first seen in E13.5 mutant embryos, and by E14, the expression is nearly completely lost (data not shown).

To determine whether the eventual absence of *Drg11* and *Ebf3* expression was caused by loss of mutant cells, we examined cell death by the TUNEL labeling method (Gavrieli et al. 1992) in embryos from E11.5 to E14.5, at 12-h intervals. At every embryonic stage examined, no increase of cell death was detected in *Rnx*/*Tlx-1* double mutants in comparison with wild-type embryos (Fig. 7, cf. C and D, arrows; data not shown). Thus, the mutant cells likely survived in *Rnx*/*Tlx-1*-double-deficient mice.

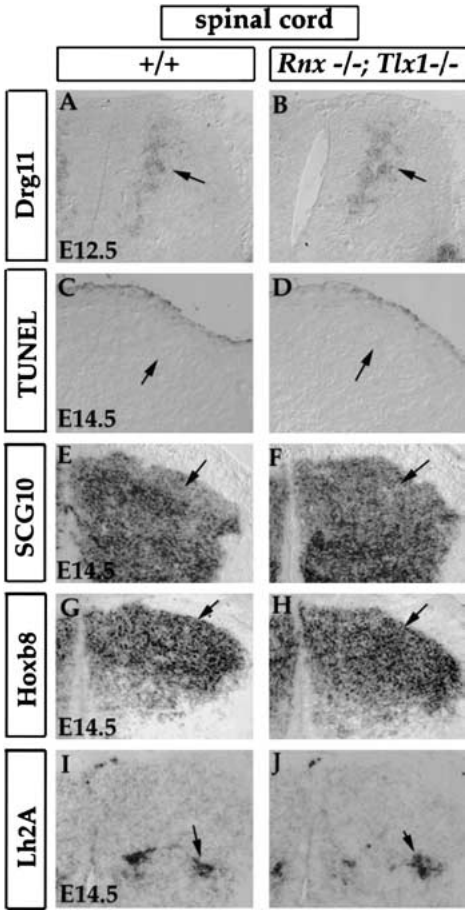

Figure 7. Mutant cells in the spinal cord survived and differentiated into dorsal horn neurons. Transverse sections through the lumbar level of the dorsal spinal cord of E12.5 (*A*,*B*) and E14.5 (*C–J*) embryos with indicated genotypes. In situ hybridization was performed with indicated probes (*A*,*B*,*E–F*). Panels *C* and *D* show TUNEL labeling in E14.5 wild-type (*C*) and double mutant embryos (*D*). No enhanced cell death was detected in E14.5 mutant embryos (cf. *C* and *D*, arrows), or in E11.5, E12, E12.5, E13, or E13.5 embryos (data not shown).

To address possible fates of the mutant cells, we examined the expression of a series of additional molecular markers. First, the mutant cells in the superficial laminae of the spinal cord apparently continued to differentiate into neuronal cells, indicated by expression of *SCG10*, a pan-neuronal marker (Stein et al. 1988), in E14.5 mutant embryos (Fig. 7, cf. E and F, arrows). Second, the mutant cells do retain certain normal features, as demonstrated by the normal expression of *Hoxb8* (Fig. 7, cf. G and H, arrows) and *neuropilin-1* (data not shown), two dorsal horn neuron markers (Graham et al. 1991; He and Tessier-Lavigne 1997; Kolodkin et al. 1997). Third, none of the deep laminar markers, including *Lh2A* (Fig. 7, cf. I and J, arrows), *Slit2* (see Fig. 9 below), and *Sema-3A* (see Fig. 9 below), show ectopic expression in the superficial laminae of *Rnx*/*Tlx* double mutants. Thus, there is no evidence indicating a fate switch from the superficial to the deep layers of neurons.

Projection defect of trkA+ afferents in Rnx *and* Tlx-1 *double mutants*

The superficial laminae of the dorsal spinal cord and Sp5 are the primary targets of trkA+ nociceptive/thermoceptive sensory afferents. The loss of expression of *Drg11* and *Ebf3* in these structures led us to examine whether central projections of trkA+ afferents are affected in *Rnx* and *Tlx-1* double mutants. Since *trkA* mRNA is expressed in the DRG and nTG (Huang et al. 1999; Huang and Reichardt 2001), but not in the spinal cord or Sp5 (data not shown), trkA immunostaining is indicative of the central projections of the nociceptive/thermoceptive sensory afferents. In E14.5 wild-type embryos, trkA+ afferents have reached the dorsal entry zone (Fig. 8A, arrowhead), and have started to make collateral branches into the spinal cord (Fig. 8A, arrow). In E14.5 *Rnx*/*Tlx-1* double mutants, trkA+ afferents are able to reach the dorsal entry zone (Fig. 8B, arrowhead), but fail to make any entry to the dorsal horn (Fig. 8B, arrow). At E18.5, ingrowth of trkA+ afferents in double mutants is much shallower in comparison with the projections seen in wild-type embryos (Fig. 8, cf. C and D, arrows). Ingrowth of cranial trkA+ afferents to the spinal-trigeminal nucleus is also compromised in *Rnx*/*Tlx-1* double mutants (Fig. 8, cf. E and F, arrows). In contrast, the projection of a subset of trkA+ afferents to the deep laminae of the spinal cord appears not to be affected in mutant embryos (Fig. 8, cf. C and D, arrowheads).

Previous in vitro studies suggest that bovine Slit2 protein is able to stimulate collateral branching of rat trkA+ sensory afferents (Wang et al. 1999). However, in E14.5 dorsal horn, *Slit2* is not expressed in the superficial laminae in wild-type embryos (Fig. 9A, asterisk), where predominant *Rnx* expression is detected (Fig. 5J). *Slit2* expression in other areas is also unperturbed in *Rnx*/*Tlx-1* double mutants, including the deep laminae (Fig. 9, cf. A and B, arrows) and the dorsal middle line (Fig. 9, cf. A and B, arrowheads). Expression of two additional *Slit* family members, *Slit-1* and *Slit-3* (Holmes et al. 1998; Itoh et al. 1998; Brose et al. 1999; Li et al. 1999; Yuan et al. 1999),

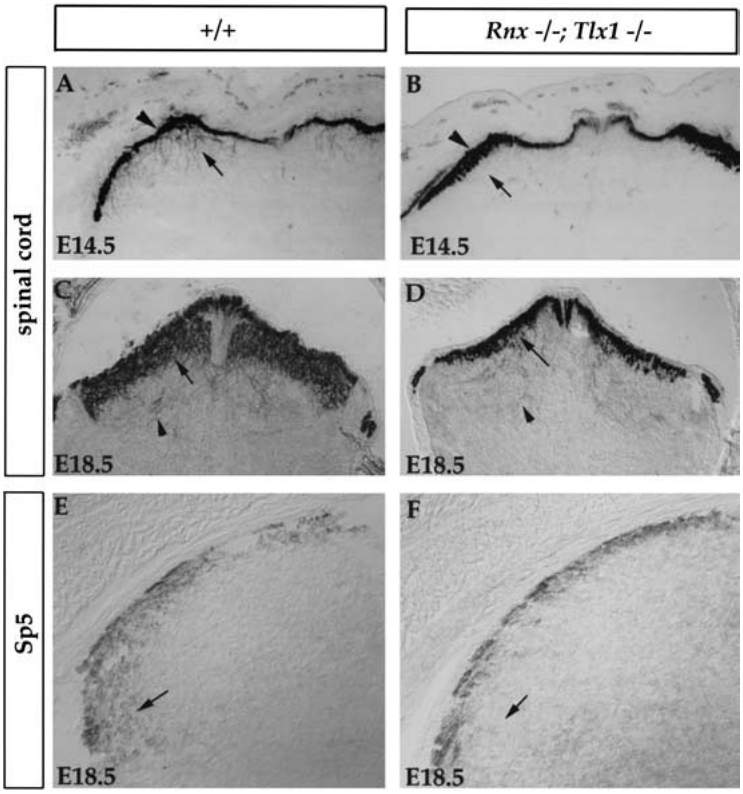

Figure 8. Defect of ingrowth of trkA+ afferents in *Rnx* and *Tlx-1* double mutants. Transverse sections through the dorsal lumbar level spinal cord (*A–D*) and the dorsal caudal medulla (*E–F*) of embryos with indicated stages and genotypes. Anti-trkA immunostaining was performed. Note, trkA afferents enter the dorsal horn in E14.5 wild-type embryos (*A*, arrow), but no entry occurs in E14.5 mutant embryos (*B*, arrow). At E18.5, much shallower projection was observed in the mutant spinal cord in comparison with wild-type embryos (cf. *C* and *D*, arrows). Similar ingrowth defect is seen in E18.5 spinal trigeminal nucleus (cf. *E* and *F*, arrows). In contrast, deep projection of trkA+ afferents are still observed in both wild-type and mutant embryos (cf. *C* and *D*, arrowheads).

is also largely normal in *Rnx*/*Tlx-1* double mutants (Fig. 9, cf. C and D; data not shown). Furthermore, expression of *Robo-1* and *Robo-2* (Kidd et al. 1998), encoding the receptors for the Slit proteins (Brose et al. 1999; Li et al. 1999), is normal in the peripheral sensory ganglia in *Rnx*/*Tlx-1* double mutants (data not shown).

In chick embryos, it has been hypothesized that dorsal restriction of trkA+ afferent projections is controlled by the repulsive signal, Sema-3A, which is expressed in the ventral two-thirds of the developing spinal cord (Shepherd et al. 1996, 1997; Fu et al. 2000). According to this hypothesis, entry failure of trkA+ afferents in *Rnx* and *Tlx* double mutants could be caused by an ectopic expression of *Sema-3A* in the dorsal horn, or by an overexpression of *neuropilin-1*, encoding the Sema-3A receptor, in the primary sensory afferent neurons. However, no abnormal expression of *Sema-3A* in the spinal cord (Fig. 9, cf. E and F) or *neuropilin-1* in the DRG (data not shown) is detected in *Rnx* and *Tlx-1* double mutants. In summary, the projection defect of trkA+ afferent is not caused by abnormal expression of *Sema-3A* or *Slit*s, or the genes encoding their receptors.

To examine whether the projection defect was caused by major morphological change in the dorsal horn, we examined the gross pattern of neuronal migration by BrdU pulse-chase labeling. We injected BrdU at E10.5, E11.5, E12.5, or E13.5, and collected and analyzed the embryos at E14.5 or E16.5. Cells going through the final cell cycle at the time when BrdU was injected will show strongest staining with anti-BrdU antibody, while those cells going through additional rounds of cell division will show weaker staining, thus providing cell birthdating and cell migration information. In wild-type embryos (at the lumbar level), cells born at E10.5 and E11.5 are primarily restricted to ventral or deep layers of the dorsal horn (Fig. 9G, arrow; data not shown). In embryos chase-labeled at E12.5, strong BrdU staining is located in the superficial laminae (Fig. 9I, arrows). Note that a weaker staining is detected in the deep medial areas (Fig. 9I, asterisk), suggesting that these cells may have gone through additional rounds of cell division. Consistently, cells born at E13.5 are primarily located in the same deep medial area (Fig. 9K, arrow). No dramatic change of BrdU-labeling is observed in *Rnx*/*Tlx-1* double mutants (Fig. 9, cf. G and H; I and J; L and K), suggesting that the gross pattern of neuronal migration might not be affected in *Rnx*/*Tlx-1*-deficient embryos.

Discussion

Possible fates of dorsal MASH1-positive precursors and origins of first-order relay sensory neurons and D2/D4 interneurons

The origins of various relay sensory neurons in the hindbrain and spinal cord is only beginning to be understood, partly due to the lack of prospective molecular markers for these neurons. Earlier studies have shown that the dorsal ventricular zone of the hindbrain and spinal cord is subdivided into three compartments, distinguished by complementary expression of the proneural proteins, Math1, NGN1/2, and MASH1 (Ma et al. 1997; Helms

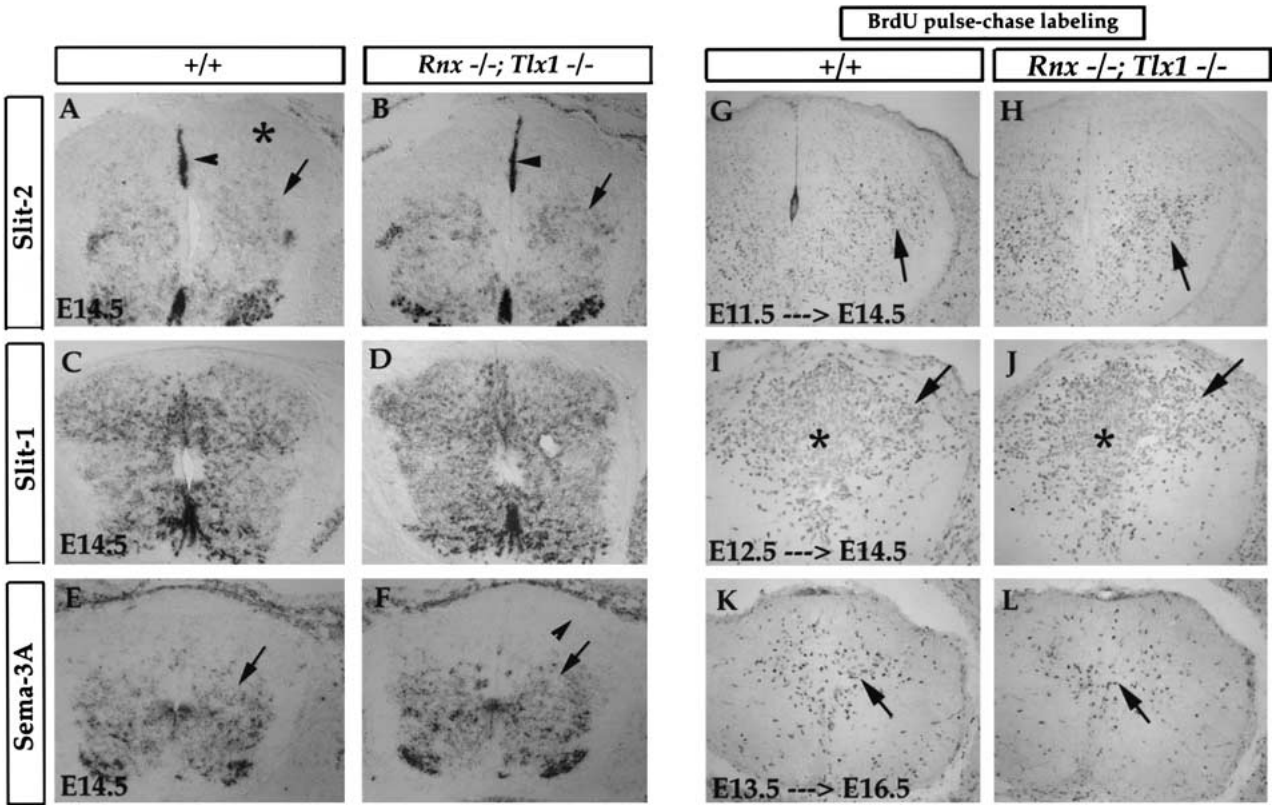

Figure 9. Expression of *Slit1/2* and *Sema-3A*, and BrdU pulse-chase labeling, in wild-type and *Rnx/Tlx-1* double mutants. Transverse sections through the spinal cord of E14.5 (*A–J*) and E16.5 (*K,L*) embryos with indicated genotypes. In situ hybridization was performed with indicated probes (*A–F*). Panels *G–L* show BrdU pulse-chase labeling. Panels *G* and *H* show embryos pulse labeled at E11.5 and analyzed at E14.5. Note, cells born at this stage are located in the ventral two-thirds of the spinal cord in both wild-type and mutant embryos (cf. *G* and *H*, arrows). Panels *I* and *J* show embryos pulse-labeled at E12.5 and analyzed at E14.5. Note, strong BrdU staining is detected in the superficial laminae in both wild-type and mutant embryos (cf. *I* and *J*, arrows). A weaker staining is observed in the deep dorsal medial area in both wild-type and mutant embryos (cf. *I* and *J*, asterisks). In embryos pulse-labeled at E13.5, BrdU staining is predominantly located in the deep medial area (*K*, arrows). Again, no gross defect was detected in *Rnx/Tlx-1* double mutants (cf. *K* and *L*, arrows).

and Johnson 1998; Lee et al. 1998; Gowan et al. 2001). Math1-positive precursors form multiple components of the proprioceptive pathway, including the pontine nucleus, cerebellum granule cells, and spinal D1 interneurons (Ben-Arie et al. 2000; Bermingham et al. 2001; Gowan et al. 2001). Dorsal NGN1/2-positive precursors form D3A interneurons in the spinal cord (Gowan et al. 2001). Our present and previous (Qian et al. 2001) studies show that the broad MASH1-positive domain appears to form a variety of *Rnx*-expressing cells, including (1) three major relay sensory stations, the nTS, the nTG, and the superficial laminae of the dorsal spinal cord; (2) two classes of dorsal interneurons, D2 and D4; and (3) brainstem (nor)adrenergic centers (summarized in Fig. 10A).

All these neurons show unique molecular identities, and are formed at distinct positions along the dorsoventral or rostrocaudal axes, or at distinct embryonic stages (Fig. 10). For example, spinal D2 interneurons, coexpressing *Rnx* and *Isl1* (Logan et al. 1998), may be formed from the most dorsal MASH1-positive domain in E10.5–E11.5 embryos (Figs. 2,3). D4 interneurons, which first express *Rnx* plus *Lmx1b* and then *Phox2a*, likely develop from the most ventral portion of MASH1-positive precursors in E10.5–E11.5 embryos (Figs. 2,4). In contrast, late born *Rnx*-positive cells appear to form from the entire dorsal MASH1-positive domain, and are fated to form the trigeminal nuclei and the superficial laminae of the dorsal spinal cord (Figs. 2,5). The fate of the intermediate portion of the MASH1-positive domain in E10.5–E11.5 embryos (Fig. 2B, arrow) remains to be determined.

The conclusion that MASH1-positive precursors may form various *Rnx*-expressing cells is based on the following observations. First, *Rnx*-expressing cells are initially located exclusively lateral to the MASH1-positive domain, and the cells at the lateral edge of the MASH1-positive domain show coexpression of *Rnx* mRNA and MASH1 protein (Fig. 2). Particularly, in E12.5 spinal cord and caudal hindbrain, there are 3–6 layers of cells showing colocalization of *Rnx* mRNA and Mash1 protein (Fig. 2G; data not shown). Second, we did not detect any adjacent NGN1-expressing cells coexpressing *Rnx* (Fig. 2H; data not shown). Third, our conclusion is consistent with the existing genetic data. For instance, the most dorsal *Phox2b* expression in the medulla, which we re-

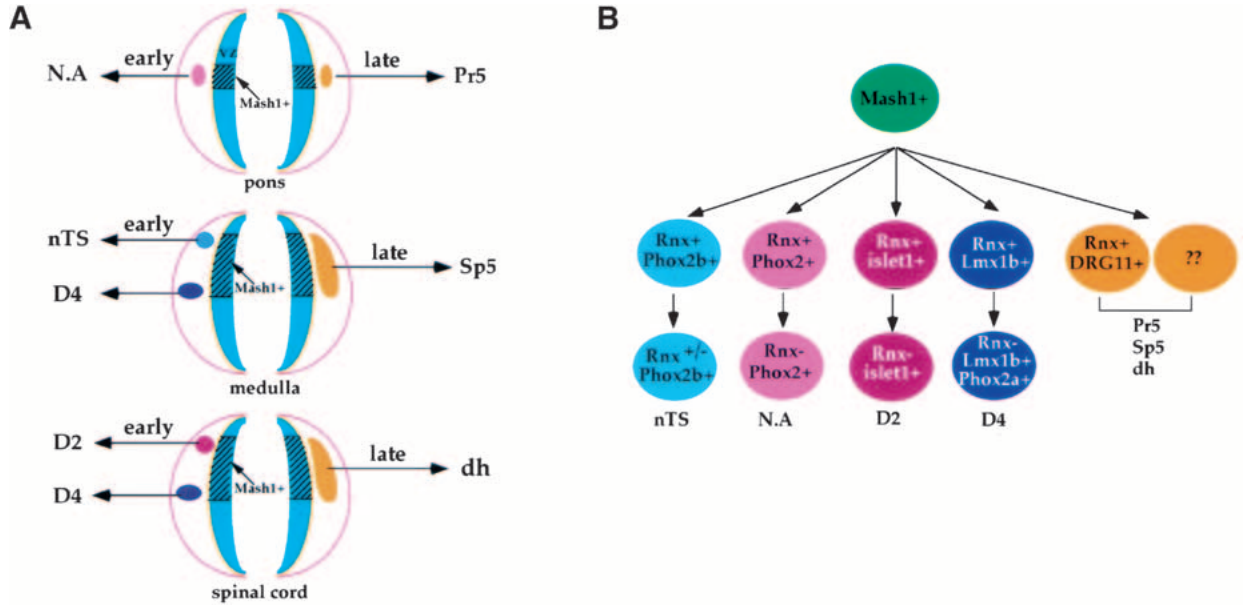

Figure 10. (*A*) Fates of dorsal *Mash1*-positive precursors and association of *Rnx* with the development of multiple classes of neurons in the hindbrain and spinal cord. The schematics show transverse sections through the pons, medulla, and spinal cord (dorsal is up). *Rnx*-expressing cells likely develop from the portion of dorsal ventricular zone (vz) that expresses the proneural gene *Mash1* (shaded regions). In the pons, early and late born *Rnx*-expressing cells are fated to form the (nor)adrenergic centers (NA) (Qian et al. 2001) and the principle trigeminal nucleus (Pr5), respectively. In the medulla and spinal cord of E10.5–E11.5 embryos (*left* panels, early), *Rnx* is expressed in two columns of cells that derive from the most dorsal and the most ventral portions of *Mash1*-positive precursors, respectively. These cells are fated to form the nucleus of solitary tract (nTS) (Qian et al. 2001) and D2/D4 interneurons (D2, D4). *Rnx* is also required for the development of medullary (nor)adrenergic centers and the area postrema (Qian et al. 2001), but precise origins of those neurons are still unclear. Late born *Rnx*-expressing cells (*right* panels, late) are formed from the entire dorsoventral extent of the *Mash1*-positive domain in the medulla and spinal cord, and are fated to become the spinal trigeminal nucleus (Sp5) and the dorsal horn of the spinal cord (dh). (*B*) Molecular identities of neurons controlled by *Rnx*. *Phox2* represents *Phox2a* or *Phox2b*. As mentioned above, all *Rnx*-positive neurons likely develop from *Mash1*-positive precursors. Note, *Rnx* expression is down-regulated in the (nor)adrenergic neurons (N.A.) (Qian et al. 2001), the caudal nTS (Qian et al. 2001; data not shown), a portion of the spinal trigeminal nucleus (Fig. 5), and spinal D4 interneurons (Fig. 4). *Rnx* expression in the spinal D2 interneurons is also transient (data not shown). In contrast, *Rnx* expression is maintained at a high level in the rostral nTS (Qian et al. 2001), portions of the Pr5 and Sp5, and the superficial laminae of the dorsal spinal cord (Fig. 5). The molecular identities of a subset of cells in the Sp5 and the dh are unclear (marked with "??").

cently identified as a prospective marker for the nTS neurons and possibly the (nor)adrenergic neurons (Qian et al. 2001), is absent in *Mash1*-deficient mice (Hirsch et al. 1998). Spinal expression of *Phox2a*, which we show here as a comarker for D4 interneurons (Fig. 4), is also absent in *Mash1* mutants (Hirsch et al. 1998). Furthermore, genetic fate mapping studies do not show any progeny cells from NGN1- and Math1-positive precursors that coexpress the D2 interneuron marker, *Isl1*, and D2 cell development is not affected in *ngn1/2*- or *Math1*-deficient mice (Bermingham et al. 2001; Gowan et al. 2001). These studies strongly suggest that *Rnx*-expressing cells develop from MASH1-positive precursors, although our data have not ruled out the formal possibility that NGN1- and Math1-positive cells might give rise to a subset of *Rnx*-expressing cells.

Our studies reveal an ontogenetic relationship between D2 interneurons and the nTS (Fig. 10). Both of them develop from the dorsal column of *Rnx*-expressing cells in E10.5–E11.5 embryos, and both appear to migrate ventrally (Fig. 3; Qian et al. 2001). The nTS is the target for trkB+ visceral sensory afferents. Interestingly, D2 interneurons are located in the deep laminae of the dorsal horn (Ozaki and Snider 1997), to which trkB+ mechanoceptive afferents are thought to project (Brown et al. 1977; Ralston et al. 1984; Shortland et al. 1989; Snider 1994). Actually, many visceral sensory neurons that project to the caudal nTS, including baroreceptors and pulmonary stretch receptors, are bona fide mechanosensory neurons (Blessing 1997). By analogy, it is possible that D2 interneurons are the targets for certain mechanoceptive somatic sensory neurons.

A central role of Rnx *and* Tlx-1 *in the formation of first-order relay somatic and rely visceral sensory neurons*

We showed previously that *Rnx* is required for proper development of the nTS, the major relay station for visceral sensory afferents (Qian et al. 2001). The defect of the nTS provides a plausible explanation for why *Rnx*-deficient mice die from a defect of breathing control

(Shirasawa et al. 2000). Here we demonstrate that *Rnx* and *Tlx-1* together are also required for proper development of most relay somatic sensory neurons, including the spinal-trigeminal nucleus (Sp5), the dorsal horn of the spinal cord, and a portion of the principle trigeminal nucleus (Pr5). The defects in *Rnx*/*Tlx-1* double mutants are indicated by the loss or reduction of expression of *Drg11*, *Ebf3*, and *Lmx1b* (Fig. 6), and by the failure of ingrowth of trkA+ nociceptive and thermoceptive afferents to the nTG and the dorsal horn of the spinal cord (Fig. 8; also see below). In addition, *Rnx* and *Tlx-1* are required for the proper formation of two classes of dorsal interneurons, D2 and D4, as indicated by the loss of *Isl1* and *Lmx1b* expression in *Rnx*/*Tlx-1* double mutants (Figs. 3,4). Thus, the Tlx family of homeobox proteins emerges as the central regulators for the development of the relay somatic and the relay visceral sensory neurons.

In the dorsal spinal cord, the mutant cells appear to migrate properly, based on the comparable BrdU pulse-chase labeling patterns in wild-type and double mutant embryos (Fig. 9), although this methodology does not rule out subtle morphological change. The mutant cells differentiate into neuronal cells, as indicated by *SCG10* expression (Fig. 7), and retain certain features for dorsal horn neurons, as demonstrated by normal expression of *Hoxb8* and *neuropilin-1* (Fig. 7; data not shown). At the molecular level, *Rnx* and *Tlx-1* may have a unique function in maintaining expression of a variety of transcription regulators. We found previously that initiation of *Phox2b* expression in the developing nTS is independent of *Rnx* (Qian et al. 2001). Here we show that initiation of *Drg11* and *Ebf3* expression in the developing nTG and the dorsal spinal cord, and the initial *Lmx1b* expression in the prospective D4 interneurons, are not affected in *Rnx*/*Tlx-1* double mutants (Figs. 4,7; data not shown). However, expression of all these genes is lost during a period when no cell death is detected by the TUNEL method (Figs. 4,6,7; Qian et al. 2001). The mechanisms by which Rnx and Tlx-1 maintain expression of a variety of molecular targets remain to be determined.

Rnx and *Tlx-1* apparently share functional redundancy. We have not observed any neuronal defects in *Tlx-1* single mutants, and the severity of abnormality in *Rnx* single mutants inversely correlates with the degree of *Tlx-1* expression in that structure. For instance, *Tlx-1* is expressed in medullary but not spinal D4 interneurons. Consequently, spinal D4 cell development is compromised in *Rnx* single mutants, while defect of medullary D4 interneuron formation only occurs in *Rnx*/*Tlx-1* double mutants (Fig. 4).

Central ingrowth of the trkA+ afferents is dependent on Rnx *and* Tlx-1

Rnx and *Tlx-1* represent the very few transcription factors identified thus far that are required for proper entry of trkA+ sensory afferents to the Sp5 and the dorsal horn of the spinal cord. The failure of ingrowth of trkA+ afferents observed in *Rnx*/*Tlx-1* double mutants is different from the projection phenotype seen in *Drg11*-deficient mice. In *Drg11* mutants, trkA+ afferents are able to make collateral entry to the dorsal spinal cord, although the projections are rerouted to the medial area (Chen et al. 2001). The difference is possibly due to the fact that besides *Drg11*, Rnx and Tlx-1 control additional targets, such as *Ebf3* and *Lmx1b*.

The cause of the trkA+ afferent ingrowth defect is still unclear. Although we have not ruled out a defect of projection neurons in the DRG and the trigeminal ganglia, several observations are more consistent with the target field defect model. Of the three *Tlx* family members, *Tlx-2* is expressed exclusively in peripheral sensory ganglia (Tang et al. 1998; data not shown), and might compensate the loss of *Tlx-1* and *Rnx*. Indeed, no abnormal neuronal differentiation is detected in the DRG and trigeminal ganglia in *Rnx*/*Tlx-1* double mutants (data not shown). This is best exemplified by the finding that *Drg11* expression is lost in the mutant dorsal spinal cord and spinal trigeminal nuclei (Fig. 6), but is normal in the DRG and trigeminal ganglia (data not shown). In addition, *Isl1* expression is absent in the spinal D2 interneurons, but normal in the DRG in *Rnx*/*Tlx-1* double mutants (Fig. 3). As mentioned above, we have no evidence indicating aberrant neuronal migration of the dorsal horn neurons. We think that the simplest interpretation is that *Rnx* and *Tlx-1* might regulate the expression of molecules that are crucial for collateral entry of sensory afferents.

Previous in vitro studies suggested that *Sema-3A* and members of the *Slit* family may control trkA+ afferent projections in the dorsal spinal cord (Puschel et al. 1996; Shepherd et al. 1997; Wang et al. 1999; Fu et al. 2000). However, expression of these signaling molecules and their receptors is largely unperturbed in *Rnx*/*Tlx-1* double mutants (Fig. 9). Thus, our studies raise the possibility that in vivo, trkA+ afferent ingrowth might be controlled by molecules other than Sema-3A or Slits. Alternatively, Rnx and Tlx-1 might regulate expression of molecules required for Sema-3A or Slit protein functions.

Are the relay somatic and the relay visceral sensory neurons phylogenetically related?

Our studies reveal significant parallels between brainstem relay somatic (nTG) and relay visceral (nTS) sensory nuclei. First, both the nTS (Qian et al. 2001) and the nTG (Figs. 4–6) likely develop from MASH1-positive neural precursors, and depend on members of the *Tlx* family of homeobox genes for proper formation. Second, *Drg11* and *Phox2b*, which are expressed in the nTG and nTS, respectively (Fig. 5; Qian et al. 2001), are closely related members of paired class homeobox genes (Saito et al. 1995; Pattyn et al. 1997). Third, regulation of *Drg11* and *Phox2b* shows remarkable similarities. As mentioned above, initiation of *Drg11* (Fig. 6) and *Phox2b* (Qian et al. 2001) expression is independent of *Rnx*. However, once the cells are in the migration pathways, expression of both genes becomes dependent on *Rnx* or *Tlx-1* (Qian et al. 2001; data not shown). These parallels

raise the possibility that brainstem relay visceral and relay somatic sensory nuclei might have evolved from a common ancestor.

Materials and methods

Animals

The generation of *Tlx-1* and *Rnx* mutant mice has been described (Roberts et al. 1994; Shirasawa et al. 2000). *Tlx-1* and *Rnx* heterozygous mice were intercrossed to generate double heterozygous mice, which were in turn intercrossed to generate double mutant embryos (*Rnx*$^{-/-}$; *Tlx-1*$^{-/-}$). The morning that vaginal plugs were observed was considered E0.5. PCR-based genotyping was performed as described (Ma et al. 2000). Wild-type *Tlx-1* allele was amplified with the following primers that produce a 0.13-kb product: HOX11P7, 5′-CTTCGGTATCGAA CAGATCC-3′ and HOX11P8, 5′-CGGAGCCCCCGCCGCCG TAAGAG-3′. Mutant *Tlx-1* allele was amplified with the following primers that produce a 0.2-kb fragment: Hox11P1, 5′-CCTCCAGGATGGAGACTATGGCC-3 and Hox11P2, 5′-GG GGAACTTCCTGACTAGGGGAG-3′. Wild-type and mutant *Rnx* alleles were genotyped with HOXL2P1, 5′-AGCGGCGAC TGCTCTCCATCCAGG-3′ and Hox11P2 (see above), which produces 0.33-kb and 0.4-kb products, respectively.

In situ hybridization and immunostaining

Section in situ hybridization was performed as described (Ma et al. 1998). Anti-trkA immunostaining was performed as described by Huang et al. (1999). In situ hybridization combined with antibody immunostaining was performed essentially as described (Tiveron et al. 1996). The following in situ probes were used: *Tlx-1*, *Enx*, and *Rnx* (Qian et al. 2001); *Phox2a* (Tiveron et al. 1996), *Phox2b* (Pattyn et al. 1997), *trkA* (Birren et al. 1993), *Lmx1b* (Chen et al. 2001), *Drg11* (Saito et al. 1995), *Slit1* (Yuan et al. 1999), *Slit2* (Yuan et al. 1999), *Slit3* (Yuan et al. 1999), *Robo1* (Brose et al. 1999; Li et al. 1999), *Robo2* (Brose et al. 1999; Li et al. 1999), *Sema-3A* (Messersmith et al. 1995), *neuropilin1* (He and Tessier-Lavigne 1997), *neuropilin2* (Kolodkin et al. 1997), and *Hoxb8* (Graham et al. 1991).

BrdU pulse-chase labeling

Pregnant wild-type mice carrying E10.5, E11.5, E12.5, and E13.5 embryos were injected with 5-bromo-2-deoxy-uridine (BrdU) (Sigma) (50 mg/kg body weight), and embryos were collected at E14.5 or E16.5, fixed overnight in 4% paraformaldehyde, sunk in 20% sucrose, and embedded in OCT (Tissue-Tek). For immunostaining on frozen sections with anti-BrdU antibody (Boehringer Mannheim) (1:50 dilution), sections were dried at 50°C for 15 min; fixed in 4% paraformaldehyde for 10 min; incubated for 2 h at 70°C in 50% formamide, 1× SSC, plus 0.1% Tween-20; 1 h at 70°C in 0.2× SSC; washed with PBS; treated with 2 N HCl in PBS for 30 min at 37°C; rinsed in PBS five times; and washed with PBS (3 × 5 min). Subsequent immunostaining with anti-BrdU antibody (Boehringer Mannheim) (1:50 dilution) was performed with a Vectastain detection kit (Vector Labs) according to the manufacturer's instructions, except that 0.001% rather than 0.003% H_2O_2 was used in the final enzymatic reaction. The slower rate of reaction prevented overstaining and made it easier to distinguish cells that have gone through the final round, or additional rounds, of cell cycle.

TUNEL staining on cryostat sections

Two pairs of E10.5–E14.5 wild-type and mutant embryos were used. The TUNEL assay on frozen sections was performed according to the ApopTag method (Intergen).

Acknowledgments

We thank Drs. Stanley Korsmeyer for providing *Rnx* and *Tlx-1*/*Hox11* knockout mice, Jean-François Brunet for the Phox2a and Phox2b antibodies, Louis Reichardt for the trkA antibody, Li-Ching Lo and David J. Anderson for the MASH1 antibody, and Jane Johnson for the NGN1 antibody. We also thank Drs. Marc Tessier-Lavigne, Yi Rao, Randy Johnson, David Anderson, Mario Capecchi, and Jane Johnson for in situ hybridization probes. We thank Drs. Bernd Fritzsch, Jane Johnson, Jeremy Green, David Rowitch, Paul Gray, Annette Ferrari, and anonymous reviewers for critical comments on the manuscript. Q.M. is a Claudia Adams Barr Investigator and a Pew Scholar in Biomedical Sciences. The work is supported by NIH grant 1 R01 DE13843-01 (Q.M.).

The publication costs of this article were defrayed in part by payment of page charges. This article must therefore be hereby marked "advertisement" in accordance with 18 USC section 1734 solely to indicate this fact.

References

Ben-Arie, N., Hassan, B.A., Bermingham, N.A., Malicki, D.M., Armstrong, D., Matzuk, M., Bellen, H.J., and Zoghbi, H.Y. 2000. Functional conservation of atonal and Math1 in the CNS and PNS. *Development* **127:** 1039–1048.

Bermingham, N.A., Hassan, B.A., Wang, V.Y., Fernandez, M., Banfi, S., Bellen, H.J., Fritzsch, B., and Zoghbi, H.Y. 2001. Proprioceptor pathway development is dependent on Math1. *Neuron* **30:** 411–422.

Birren, S.J., Lo, L.C., and Anderson, D.J. 1993. Sympathetic neurons undergo a developmental switch in trophic dependence. *Development* **119:** 597–610.

Blessing, W.W.1997. *The lower brainstem and body homeostasis*. Oxford University Press, New York, NY.

Brose, K., Bland, K.S., Wang, K.H., Arnott, D., Henzel, W., Goodman, C.S., Tessier-Lavigne, M., and Kidd, T. 1999. Slit proteins bind Robo receptors and have an evolutionarily conserved role in repulsive axon guidance. *Cell* **96:** 795–806.

Brown, A.G., Rose, P.K., and Snow, P.J. 1977. The morphology of hair follicle afferent fibre collaterals in the spinal cord of the cat. *J. Physiol.* **272:** 779–797.

Chen, Z.F., Rebelo, S., White, F., Malmberg, A.B., Baba, H., Lima, D., Woolf, C.J., Basbaum, A.I., and Anderson, D.J. 2001. The paired homeodomain protein DRG11 is required for the projection of cutaneous sensory afferent fibers to the dorsal spinal cord. *Neuron* **31:** 59–73.

Davies, A.M. 1988. The trigeminal system: An advantageous experimental model for studying neuronal development. *Development* **103:** 175–183.

Dear, T.N., Sanchez-Garcia, I., and Rabbitts, T.H. 1993. The *HOX11* gene encodes a DNA-binding nuclear transcription factor belonging to a distinct family of homeobox genes. *Proc. Natl. Acad. Sci.* **90:** 4431–4435.

Dear, T.N., Colledge, W.H., Carlton, M.B., Lavenir, I., Larson, T., Smith, A.J., Warren, A.J., Evans, M.J., Sofroniew, M.V., and Rabbitts, T.H. 1995. The *Hox11* gene is essential for cell survival during spleen development. *Development* **121:** 2909–2915.

Dube, I.D., Kamel-Reid, S., Yuan, C.C., Lu, M., Wu, X., Corpus, G., Raimondi, S.C., Crist, W.M., Carroll, A.J., Minowada, J., et al. 1991. A novel human homeobox gene lies at the chromosome 10 breakpoint in lymphoid neoplasias with chromosomal translocation t10;14. *Blood* **78:** 2996–3003.

Fu, S.Y., Sharma, K., Luo, Y., Raper, J.A., and Frank, E. 2000. SEMA3A regulates developing sensory projections in the chicken spinal cord. *J. Neurobiol.* **45:** 227–236.

Garel, S., Marin, F., Mattei, M.G., Vesque, C., Vincent, A., and Charnay, P. 1997. Family of *Ebf/Olf-1*-related genes potentially involved in neuronal differentiation and regional specification in the central nervous system. *Dev. Dyn.* **210:** 191–205.

Gavrieli, Y., Sherman, Y., and Ben-Sasson, S.A. 1992. Identification of programmed cell death in situ via specific labeling of nuclear DNA fragmentation. *J. Cell Biol.* **119:** 493–501.

Gowan, K., Helms, A.W., Hunsaker, T.L., Collisson, T., Ebert, P.J., Odom, R., and Johnson, J.E. 2001. Crossinhibitory activities of Ngn1 and Math1 allow specification of distinct dorsal interneurons. *Neuron* **31:** 219–232.

Graham, A., Maden, M., and Krumlauf, R. 1991. The murine *Hox-2* genes display dynamic dorsoventral patterns of expression during central nervous system development. *Development* **112:** 255–264.

Hatano, M., Roberts, C.W., Minden, M., Crist, W.M., and Korsmeyer, S.J. 1991. Deregulation of a homeobox gene, *HOX11*, by the t10;14 in T cell leukemia. *Science* **253:** 79–82.

Hatano, M., Aoki, T., Dezawa, M., Yusa, S., Iitsuka, Y., Koseki, H., Taniguchi, M., and Tokuhisa, T. 1997. A novel pathogenesis of megacolon in *Ncx/Hox11L.1* deficient mice. *J. Clin. Invest.* **100:** 795–801.

He, Z. and Tessier-Lavigne, M. 1997. Neuropilin is a receptor for the axonal chemorepellent Semaphorin III. *Cell* **90:** 739–751.

Helms, A.W. and Johnson, J.E. 1998. Progenitors of dorsal commissural interneurons are defined by MATH1 expression. *Development* **125:** 919–928.

Hirsch, M.R., Tiveron, M.C., Guillemot, F., Brunet, J.F., and Goridis, C. 1998. Control of noradrenergic differentiation and Phox2a expression by MASH1 in the central and peripheral nervous system. *Development* **125:** 599–608.

Holmes, G.P., Negus, K., Burridge, L., Raman, S., Algar, E., Yamada, T., and Little, M.H. 1998. Distinct but overlapping expression patterns of two vertebrate slit homologs implies functional roles in CNS development and organogenesis. *Mech. Dev.* **79:** 57–72.

Huang, E.J. and Reichardt, L.F. 2001. Neurotrophins: Roles in neuronal development and function. *Annu. Rev. Neurosci.* **24:** 677–736.

Huang, E.J., Wilkinson, G.A., Fariñas, I., Backus, C., Zang, K., Wong, S.L., and Reichardt, L.F. 1999. Expression of trk receptors in the developing mouse trigeminal ganglion: In vivo evidence for NT-3 activation of trkA and trkB in addition to trkC. *Development* **126:** 2191–2203.

Itoh, A., Miyabayashi, T., Ohno, M., and Sakano, S. 1998. Cloning and expressions of three mammalian homologues of *Drosophila* slit suggest possible roles for Slit in the formation and maintenance of the nervous system. *Brain Res. Mol. Brain Res.* **62:** 175–186.

Kennedy, M.A., Gonzalez-Sarmiento, R., Kees, U.R., Lampert, F., Dear, N., Boehm, T., and Rabbitts, T.H. 1991. *HOX11*, a homeobox-containing T-cell oncogene on human chromosome 10q24. *Proc. Natl. Acad. Sci.* **88:** 8900–8904.

Kidd, T., Russell, C., Goodman, C.S., and Tear, G. 1998. Dosage-sensitive and complementary functions of roundabout and commissureless control axon crossing of the CNS midline. *Neuron* **20:** 25–33.

Kolodkin, A.L., Levengood, D.V., Rowe, E.G., Tai, Y.T., Giger, R.J., and Ginty, D.D. 1997. Neuropilin is a semaphorin III receptor. *Cell* **90:** 753–762.

Lee, K.J., Mendelsohn, M., and Jessell, T.M. 1998. Neuronal patterning by BMPs: A requirement for GDF7 in the generation of a discrete class of commissural interneurons in the mouse spinal cord. *Genes & Dev.* **12:** 3394–3407.

Li, H.S., Chen, J.H., Wu, W., Fagaly, T., Zhou, L., Yuan, W., Dupuis, S., Jiang, Z.H., Nash, W., Gick, C., et al. 1999. Vertebrate slit, a secreted ligand for the transmembrane protein roundabout, is a repellent for olfactory bulb axons. *Cell* **96:** 807–818.

Liem, Jr., K.F., Tremmel, G., and Jessell, T.M. 1997. A role for the roof plate and its resident TGFβ-related proteins in neuronal patterning in the dorsal spinal cord. *Cell* **91:** 127–138.

Logan, C., Wingate, R.J.T., McKay, I.J., and Lumsden, A. 1998. *Tlx-1* and *Tlx-3* homeobox gene expression in cranial sensory ganglia and hindbrain of the chick embryo: Markers of patterned connectivity. *J. Neurosci.* **18:** 5389–5402.

Ma, Q., Sommer, L., Cserjesi, P., and Anderson, D.J. 1997. *Mash1* and *neurogenin1* expression patterns define complementary domains of neuroepithelium in the developing CNS and are correlated with regions expressing Notch ligands. *J. Neurosci.* **17:** 3644–3652.

Ma, Q., Chen, Z.F., Barrantes, I.B., de la Pompa, J.L., and Anderson, D.J. 1998. *Neurogenin 1* is essential for the determination of neuronal precursors for proximal cranial sensory ganglia. *Neuron* **20:** 469–482.

Ma, Q., Anderson, D.J., and Ftitzsch, B. 2000. *Neurogenin1* null mutant ears develop fewer, morphologically normal hair cells in smaller sensory epithelia devoid of innervation. *J. Assoc. Res. Otolaryngol.* **1:** 129–143.

Messersmith, E.K., Leonardo, E.D., Shatz, C.J., Tessier-Lavigne, M., Goodman, C.S., and Kolodkin, A.L. 1995. Semaphorin III can function as a selective chemorepellent to pattern sensory projections in the spinal cord. *Neuron* **14:** 949–959.

Moran-Rivard, L., Kagawa, T., Saueressig, H., Gross, M.K., Burrill, J., and Goulding, M. 2001. Evx1 is a postmitotic determinant of v0 interneuron identity in the spinal cord. *Neuron* **29:** 385–399.

Ozaki, S. and Snider, W.D. 1997. Initial trajectories of sensory axons toward laminar targets in the developing mouse spinal cord. *J. Comp. Neurol.* **380:** 215–229.

Pattyn, A., Morin, X., Cremer, H., Goridis, C., and Brunet, J.-F. 1997. Expression and interactions of the two closely related homeobox genes *Phox2a* and *Phox2b* during neurogenesis. *Development* **124:** 4065–4075.

Pierani, A., Moran-Rivard, L., Sunshine, M.J., Littman, D.R., Goulding, M., and Jessell, T.M. 2001. Control of interneuron fate in the developing spinal cord by the progenitor homeodomain protein Dbx1. *Neuron* **29:** 367–384.

Puschel, A.W., Adams, R.H., and Betz, H. 1996. The sensory innervation of the mouse spinal cord may be patterned by differential expression of and differential responsiveness to semaphorins. *Mol. Cell. Neurosci.* **7:** 419–431.

Qian, Y., Fritzsch, B., Shirasawa, S., Chen, C.L., Choi, Y., and Ma, Q. 2001. Formation of brainstem noradrenergic centers and first-order relay visceral sensory neurons is dependent on homeodomain protein Rnx/Tlx3. *Genes & Dev.* **15:** 2533–2545.

Raju, K., Tang, S., Dube, I.D., Kamel-Reid, S., Bryce, D.M., and Breitman, M.L. 1993. Characterization and developmental expression of *Tlx-1*, the murine homolog of *HOX11*. *Mech. Dev.* **44:** 51–64.

Ralston III, H.J., Light, A.R., Ralston, D.D., and Perl, E.R. 1984. Morphology and synaptic relationships of physiologically

identified low-threshold dorsal root axons stained with intra-axonal horseradish peroxidase in the cat and monkey. *J. Neurophysiol.* **51:** 777–792.

Roberts, C.W., Shutter, J.R., and Korsmeyer, S.J. 1994. Hox11 controls the genesis of the spleen. *Nature* **368:** 747–749.

Saito, T., Greenwood, A., Sun, Q., and Anderson, D.J. 1995. Identification by differential RT-PCR of a novel paired homeodomain protein specifically expressed in sensory neurons and a subset of their CNS targets. *Mol. Cell. Neurosci.* **6:** 280–292.

Saper, C.B. 2000. Brain stem, reflexive behavior, and the cranial nerves. In *Principles of neural science* (eds. E.R. Kandel, J.H. Schwartz and T.M. Jessell), pp. 873–888. Mcgraw-Hill, New York, NY.

Shepherd, I., Luo, Y., Raper, J.A., and Chang, S. 1996. The distribution of *collapsin-1* mRNA in the developing chick nervous system. *Dev. Biol.* **173:** 185–199.

Shepherd, I.T., Luo, Y., Lefcort, F., Reichardt, L.F., and Raper, J.A. 1997. A sensory axon repellent secreted from ventral spinal cord explants is neutralized by antibodies raised against collapsin-1. *Development* **124:** 1377–1385.

Shirasawa, S., Yunker, A.M., Roth, K.A., Brown, G.A., Horning, S., and Korsmeyer, S.J. 1997. *Enx Hox11L1*-deficient mice develop myenteric neuronal hyperplasia and megacolon. *Nat. Med.* **3:** 646–650.

Shirasawa, S., Arata, A., Onimaru, H., Roth, K.A., Brown, G.A., Horning, S., Arata, S., Okumura, K., Sasazuki, T., and Korsmeyer, S.J. 2000. *Rnx* deficiency results in congenital central hypoventilation. *Nat. Genet.* **24:** 287–290.

Shortland, P., Woolf, C.J., and Fitzgerald, M. 1989. Morphology and somatotopic organization of the central terminals of hindlimb hair follicle afferents in the rat lumbar spinal cord. *J. Comp. Neurol.* **289:** 416–433.

Snider, W.D. 1994. Functions of the neurotrophins during nervous system development—What the knockouts are teaching us. *Cell* **77:** 627–638.

Stein, R., Orit, S., and Anderson, D.J. 1988. The induction of a neural-specific gene, *SCG10*, by nerve growth factor in PC12 cells is transcriptional, protein synthesis dependent, and glucocorticoid inhibitable. *Dev. Biol.* **127:** 316–325.

Tang, S.J., Hoodless, P.A., Lu, Z., Breitman, M.L., McInnes, R.R., Wrana, J.L., and Buchwald, M. 1998. The *Tlx-2* homeobox gene is a downstream target of BMP signalling and is required for mouse mesoderm development. *Development* **125:** 1877–1887.

Tiveron, M.-C., Hirsch, M.-R., and Brunet, J.-F. 1996. The expression pattern of the transcription factor Phox2a delineates synaptic pathways of the autonomic nervous system. *J. Neurosci.* **16:** 7649–7660.

Tsuchida, T., Ensini, M., Morton, S.B., Baldassare, M., Edlund, T., Jessell, T.M., and Pfaff, S.L. 1994. Topographic organization of embryonic motor neurons defined by expression of LIM homeobox genes. *Cell* **79:** 957–970.

Valarché, I., Tissier-Seta, J.-P., Hirsch, M.-R., Martinez, S., Goridis, C., and Brunet, J.-F. 1993. The mouse homeodomain protein Phox2 regulates *NCAM* promoter activity in concert with Cux/CDP and is a putative determinant of neurotransmitter phenotype. *Development* **119:** 881–896.

Wang, K.H., Brose, K., Arnott, D., Kidd, T., Goodman, C.S., Henzel, W., and Tessier-Lavigne, M. 1999. Biochemical purification of a mammalian slit protein as a positive regulator of sensory axon elongation and branching. *Cell* **96:** 771–784.

Wang, S.S., Tsai, R.Y.L., and Reed, R.L. 1997. The characterization of the Olf-1/EBF-like HLH transcription factor family: Implications in olfactory gene regulation and neuronal development. *J. Neurosci.* **17:** 4149–4158.

Yokoyama, M., Nishi, Y., Yoshii, J., Okubo, K., and Matsubara, K. 1996. Identification and cloning of neuroblastoma-specific and nerve tissue-specific genes through compiled expression profiles. *DNA Res.* **3:** 311–320.

Yuan, W., Zhou, L., Chen, J.H., Wu, J.Y., Rao, Y., and Ornitz, D.M. 1999. The mouse SLIT family: Secreted ligands for ROBO expressed in patterns that suggest a role in morphogenesis and axon guidance. *Dev. Biol.* **212:** 290–306.